JOC The Journal of Organic Chemistry

Article

pubs.acs.org/joc

Water-Assisted Self-Photoredox of 3-(Hydroxymethyl)benzophenone: An Unusual Photochemistry Reaction in Aqueous Solution

Xuebo Chen,*[,†] Qiangqiang Zhang,[†] Yanchang Xu,[†] Weihai Fang,*[,†] and David Lee Phillips*[,‡]

[†]Key Laboratory of Theoretical and Computational Photochemistry of Ministry of Education, Department of Chemistry, Beijing Normal University, Xin-wai-da-jie No. 19, Beijing 100875, People's Republic of China

[‡]Department of Chemistry, The University of Hong Kong, Hong Kong, People's Republic of China

Supporting Information

ABSTRACT: An unusual photochemistry of water-assisted self-photoredox of 3-(hydroxymethyl) benzophenone **1** has been investigated by CASPT2//CASSCF computations. The water-assisted self-photoredox is found to proceed via three sequential reactions: an excited-state intermolecular proton transfer (ESIPT), a photoinduced deprotonation, and a self-redox reaction. Upon photoexcitation at 243 nm, the system of **1** is taken to the Franck−Condon region of a short-distance charge transfer (SCT) state of $S_{SCT}(^1\pi\pi^*)$ and then undergoes ESIPT with a small barrier of ∼3.4 kcal/mol producing the intermediate **2**. Subsequently, the singlet−triplet crossing (STC) of STC ($^1\pi\pi^*/^3\pi\pi^*$) relays **2** by intersystem crossing to the $T_{SCT}(^3\pi\pi^*)$ state followed by a deprotonation reaction overcoming a moderate barrier of ∼8.0 kcal/mol and finally produces the triplet biradical intermediate **3**. Another moderate barrier (∼5.8 kcal/mol) in the $T_{SCT}(^3\pi\pi^*)$ state has to be overcome so as to relax to a second singlet−triplet crossing STC(T/S_0) that allows an efficient spin-forbidden decay to the ground state. The self-redox reaction aided by water molecules occurs with tiny barriers in the S_0 state via two steps, protonation of the benzhydrol carbon to produce intermediate **4** and then deprotonation from the benzylic oxygen to yield the final product 3-formylbenzhydrol **5**.

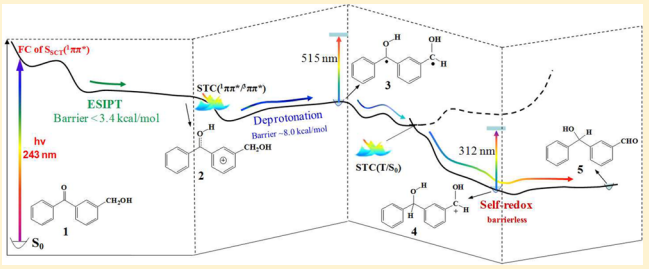

INTRODUCTION

Benzophenone (BP) and many of its derivatives have been observed to undergo typical photochemical reactions that include Norrish type I and type II, intermolecular hydrogen abstraction, and photoinduced electron transfer processes under a variety of conditions.[1−9] A new kind of photochemistry associated with meta-substituted BP was reported by Wan and co-workers, where an intramolecular photoredox reaction reduces the ketone moiety to its alcohol, and the meta-substituted alcohol group is oxidized to its aldehyde (or ketone).[10−13] The reinforced electronic communication between the 1,3-positions of the benzene ring and apparent water participation were found to be essential to the occurrence of this unusual reaction.[11,14] These findings altered the traditionally held thinking that BPs were used mainly as hydrogen abstractors or triplet sensitizers. The 3-(hydroxymethyl)benzophenone (**1**) compound used as a prime example in these studies undergoes a highly efficient ($\Phi \approx 0.6$) intramolecular photoredox reaction in acidic (pH < 3) aqueous solution to produce the predominate 3-formylbenzhydrol (**5**) (95%) and trace amounts of 3-formylbenzophenone (**6**) (5%) (see Scheme 1).[10−12]

A transient spectrum exhibiting two bands with maxima at 325 and 525 nm was observed by laser flash photolysis of **1** in 1:1 H_2O-CH_3CN, and these bands were suspected to be related to a triplet excited state intermediate.[11,15,16] Decreasing the pH of the solution led to significant quenching of this transient species ($\tau_{(pH\ 7)} = 9.5\ \mu s$, $\tau_{(pH\ 2)} = 60$ ns). This strongly suggested that the protonated triplet state could give rise to the observed photoredox products under acidic conditions.[11] Beside this, Phillips and co-workers[17] detected a new triplet biradical intermediate for the above reaction that had characteristic Raman bands at 962 and 1518 cm^{-1} in time-resolved resonance Raman (TR^3) experiments and proposed that this species was a key intermediate in this novel water-assisted photoredox reaction.

Scheme 1. Water-Assisted Self-Photoredox Reaction of 1 in Acidic (pH < 3) Aqueous Solution

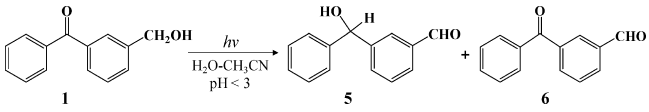

Experimental studies on the photoredox reaction of **1** over the past several years have provided some important

Received: April 24, 2013
Published: May 14, 2013

 © 2013 American Chemical Society dx.doi.org/10.1021/jo4008783 | J. Org. Chem. 2013, 78, 5677−5684

information concerning the reactive intermediates.[11−17] Several possible reactive intermediates and mechanisms have been proposed, but it has been difficult to obtain a definitive conclusion due to the strong overlap among the complicated transient spectra.[17−22] A detailed understanding of the mechanistic photochemistry of any system needs experimental investigations and theoretical calculations for the structures and reactivity of the ground and excited electronic states.[23] However, to our knowledge, there are few if any reports that involve *ab initio* studies for theoretical investigation of the photoredox reaction of **1** in aqueous solution. In our previous studies,[23−27] high-level electronic structure calculations provided detailed information concerning the Franck−Condon (FC) excitation, the intermediate, and products, as well as relaxation pathways of photoremovable protecting group (PPG) compounds that may then be compared in a quantitative manner with experimental observations. Herein, the same CASPT2//CASSCF approach will be employed to explicitly describe the properties of various transitions in the FC region and the nature of the reactive intermediates and to explain how the photoredox reaction of **1** takes place. The structures and relative energies of the lowest electronic states, as well as the mechanistic details for the photoredox reaction of **1** in aqueous solution, are characterized in this work.

COMPUTATIONAL METHODS

To mimic the water-assisted photoredox reaction of **1** in acidic aqueous solution, five water molecules were introduced to function as different roles as shown in the section 1 of Supporting Information. The complete active space self-consistent field (CASSCF) method[28] was used to optimize stationary structures on the different electronic states of **1**. Fourteen electrons in 11 orbitals were chosen as the active space for the present CASSCF calculations, referred to as CAS(14e/11o) hereafter. All these orbitals in active space are schematically shown in the Supporting Information as Figure S3 of section 5. The state-averaged CASSCF method[29] was taken to determine the geometry of the intersection space of the two electronic states with the same spin multiplicity, while the minimum-energy crossing points between the singlet and triplet states were optimized by using Slater determinants in the state-averaged CASSCF calculations. The constrained energy profiles (CEPs) of the three sequential reactions for the water-assisted self-photoredox of **1** were computed by stepwise optimizations along selected internal coordinates. For every stationary point optimization, the reaction coordinate was fixed at a given value while the other degrees of freedom were totally relaxed without any constraint. The CEPs were preliminarily mapped along the variant values of the reaction coordinate that was defined by the donor/acceptor distance for the proton transfer. To consider the dynamical electron correlation effects for these points, the refined single-point energy was recalculated at the multiconfiguration second-order perturbation theory level (CASPT2)[30] using a five roots state averaged CASSCF (14e/11o). The 6-31G* basis set was used for all CASSCF and CASPT2 calculations. All calculations in this work were performed by using Gaussian 03[31] and Molcas[32] program packages. For more computational details see the section 1 of Supporting Information.

RESULTS AND DISCUSSION

Vertical Excitation of 3-(Hydroxymethyl)-benzophenone·5H$_2$O. Table 1 summarizes the vertical excitation energies (ΔE, kcal/mol), excitation wavelength (λ, nm), oscillator strengths (f), and dipole moments (DM, debye) of different transitions for the 3-(hydroxymethyl)-benzophenone·5H$_2$O (**1**·5H$_2$O) complex. The lowest excited state of the n → π^* (NP) transition originates from the promotion of one electron of the O(2) lone pair to a π^* orbital

Table 1. Vertical Excitation Energies (ΔE, kcal/mol), Excitation Wavelength (λ, nm), oscillator strengths (f), and Dipole Moments (DM, debye) at the FC Minimum Geometric Structure for 1·5H$_2$O Complex at the CASPT2//CASSCF(14e/11o)/6-31G* Level of Theory and the Character of Singly Occupied Orbitals for the Different Transitions

Transitions	DM	f	ΔE	λ
S_0	14.80		0.0	
$S_0 \rightarrow S_{NP}(^1n\pi^*)$	16.62	0.00151	93.7	305
$S_0 \rightarrow S_{Bz}(^1\pi\pi^*)$	14.76	0.00361	98.9	289
$S_0 \rightarrow S_{SCT}(^1\pi\pi^*)$	13.33	0.449	117.9	243
$S_0 \rightarrow S_{LCT}(^1\pi\pi^*)$	11.51	0.234	117.3	244

character of singly occupied orbitals

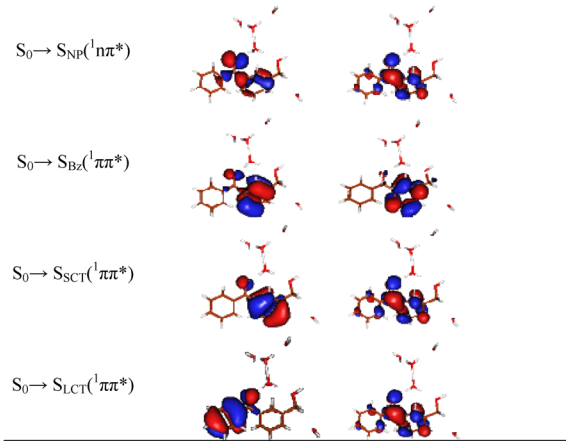

that is delocalized along the whole benzoyl (Bz) chromophore. The oscillator strength of the $S_0 \rightarrow S_{NP}(^1n\pi^*)$ transition is 0.00151 and is ∼300 times smaller than that of the maximum f. This confirms a "dark" spectroscopic property for the n → π^* transition, which is a common feature for compounds containing the Bz chromophore.[23−27] The vertical excitation energy to the $^1n\pi^*$ state is 93.7 kcal/mol, which is ∼10.0 kcal/mol higher than that of BP-containing compounds without water involved due to the formation of hydrogen bond(s) around the carbonyl O.[23−25] As illustrated in Table 1, another dark state, $S_{Bz}(^1\pi\pi^*)$ (f = 0.00361), was found to have a 98.9 kcal/mol vertical excitation energy. An electronic population analysis shows $S_0 \rightarrow S_{Bz}(^1\pi\pi^*)$ is a localized excitation in the aromatic ring, which is confirmed by a small dipole moment change (Δ = −0.04 D) in comparison with that of the S_0 state.

In contrast with this, large dipole moment changes were observed in the $S_0 \rightarrow S_{SCT}(^1\pi\pi^*)$ (Δ = −1.47 D) and the long-distance charge transfer (LCT) transition of $S_0 \rightarrow S_{LCT}(^1\pi\pi^*)$ (Δ = −3.29 D) that exhibit charge transfer character. Like the case of ketoprofen[23] and 3′,5′-dimethoxybenzoin,[24] as well as o-acetylphenylacetic acid,[25] the short-distance CT state of $S_{SCT}(^1\pi\pi^*)$ for the **1**·5H$_2$O complex was calculated to have a maximum oscillator strength (f = 0.449) over other transitions. The $S_0 \rightarrow S_{SCT}(^1\pi\pi^*)$ transition is localized at one chromophore, where the charge transfer occurs from the aromatic ring of the phenylcarbinol to the C(1)═O(2) carbonyl group, leading to an abundant gathering of negative charge around the center of the carbonyl group that can

dx.doi.org/10.1021/jo4008783 | J. Org. Chem. 2013, 78, 5677−5684

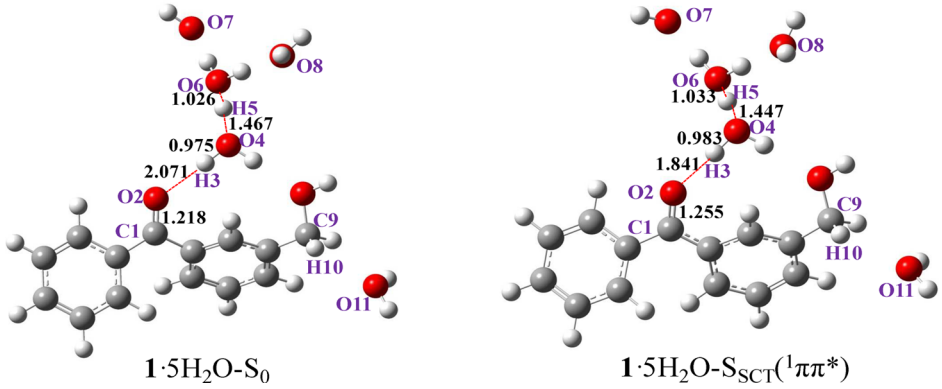

Figure 1. Schematic minimum structures for the **1**·5H_2O complex in the S_0 and $S_{SCT}(^1\pi\pi^*)$ electronic states, along with selected bond parameters (bond lengths in Å) at the CAS(14e/11o)/6-31G* level of theory.

function as a potential acceptor for a proton transfer.[23,25] As shown in Table 1, the vertical excitation energy of the $S_0 \rightarrow S_{SCT}(^1\pi\pi^*)$ transition for **1**·5H_2O is 117.9 kcal/mol and is very close to the calculated value (118.9 kcal/mol) for the same excitation for ketoprofen with two H_2O complex (KP·2H_2O)[23] but is 5.0−7.0 kcal/mol lower than that of bare ketoprofen[23] and *o*-acetylphenylacetic acid[25] molecules without the formation of hydrogen bonding with H_2O.[23] The calculated vertical excitation energy for the $S_0 \rightarrow S_{SCT}(^1\pi\pi^*)$ transition (~243 nm) with a large oscillator strength is consistent with the experimental absorption spectral band at λ_{max} = 255 nm.[11] It should be noted that the present model for the hydrogen bonding is simplified and more hydrogen bonds surrounding the C1═O2 carbonyl group are expected to exist in the actual aqueous environment, thereby leading to a lower vertical energy to the $S_{SCT}(^1\pi\pi^*)$ state than for the 3-(hydroxymethyl)-benzophenone−water complex calculated here. The mutual attraction interaction between the C1═O2 carbonyl group and the water molecules facilitates the electron migration from the benzene ring to the carbonyl group moiety [$S_0 \rightarrow S_{SCT}(^1\pi\pi^*)$ transition] but exerts an unfavorable influence on the electron promotion from the lone pair of the carbonyl O atom to the π^* of the benzene ring [$S_0 \rightarrow S_{NP}(^1n\pi^*)$ excitation]. This partially accounts for why the red-shifted $S_0 \rightarrow S_{SCT}(^1\pi\pi^*)$ and the blue-shifted $S_0 \rightarrow S_{NP}(^1n\pi^*)$ absorptions were found for aromatic carbonyl compounds when the participation with the hydrogen bonding of water molecule occurs.

Unlike the one chromophore localized charge transfer state of $S_{SCT}(^1\pi\pi^*)$, another excited state denoted as $S_{LCT}(^1\pi\pi^*)$ was observed in the FC excitation of **1**·5H_2O. The electronic population analyses concluded that the $S_0 \rightarrow S_{LCT}(^1\pi\pi^*)$ transition originates in electron promotion from one chromophore to another one via a long-distance charge transfer. As depicted in Table 1, two singly occupied electrons distribute into the two chromophores, respectively, and the $S_0 \rightarrow S_{LCT}(^1\pi\pi^*)$ transition exhibits a large change in the dipole moment. This indicates that $S_{LCT}(^1\pi\pi^*)$ will unlikely function as a precursor state for the subsequent ESIPT reaction, since the potential acceptor of the proton transfer of the carbonyl group does not get involved in this excitation pattern. Although the $S_0 \rightarrow S_{LCT}(^1\pi\pi^*)$ transition has almost the same excitation energy (117.3 kcal/mol) as that of the $S_0 \rightarrow S_{SCT}(^1\pi\pi^*)$ transition, its oscillator strength (f = 0.234) is almost half smaller than that of the $S_0 \rightarrow S_{SCT}(^1\pi\pi^*)$ excitation. Therefore, the $S_0 \rightarrow S_{SCT}(^1\pi\pi^*)$ transition has a higher possibility of initial population than the $S_0 \rightarrow S_{LCT}(^1\pi\pi^*)$ excitation upon 243 nm photoexcitation. Therefore, the $S_0 \rightarrow S_{SCT}(^1\pi\pi^*)$ transition is responsible for most of the initial population under experimental conditions.[11,17]

Photoinduced Protonation Reaction via Excited-State Intermolecular Proton Transfer. The CAS(14e/11o)/6-31G* optimized structures for the **1**·5H_2O complex in the S_0 and $S_{SCT}(^1\pi\pi^*)$ electronic states are schematically shown in Figure 1 along with selected bond parameters. Figure 2 shows

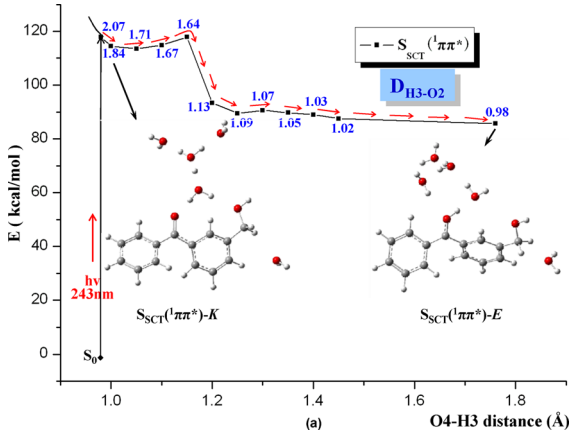

Figure 2. CEP of intermolecular proton transfer for **1** along reaction coordinate of O(4)−H(3) [or H(3)−O(2)] distance obtained at the CASPT2//CAS(14e/11o)/6-31G* level of theory. The $S_{SCT}(^1\pi\pi^*)$-*K* denotes the local minimum of the $S_{SCT}(^1\pi\pi^*)$ state in its keto form, and $S_{SCT}(^1\pi\pi^*)$-*E* stands for this state in its enol form.

the CEP of the intermolecular proton transfer of **1** from the aqueous solution. As shown in Figure 1, upon electronic excitation to the $S_{SCT}(^1\pi\pi^*)$ state, the most striking change in the complex is associated with the O(2)···H(3) distance, which is 2.071 Å in **1**·5H_2O-S_0 and becomes 1.841 Å in the **1**·5H_2O-$S_{SCT}(^1\pi\pi^*)$ structure. As pointed out before, the $S_0 \rightarrow S_{SCT}(^1\pi\pi^*)$ transition leads to the concentration of negative charge around the C(1)−O(2) carbonyl group. The O(2)···H(3) hydrogen bond is significantly strengthened due to the increase of electron density on the O(2) atom for the $S_0 \rightarrow S_{SCT}(^1\pi\pi^*)$ transition. As a result, the O(2)···H(3) distance is obviously shortened in the **1**·5H_2O-$S_{SCT}(^1\pi\pi^*)$, as compared with that in the S_0 state. Similar structural changes are associated with the distances of H(3)−O(4), O(4)···H(5), and H(5)−O(6). The elongation of the H(5)−O(6) and H(3)−O(4) bonds, together with the shortening of the O(2)···H(3)

dx.doi.org/10.1021/jo4008783 | J. Org. Chem. 2013, 78, 5677−5684

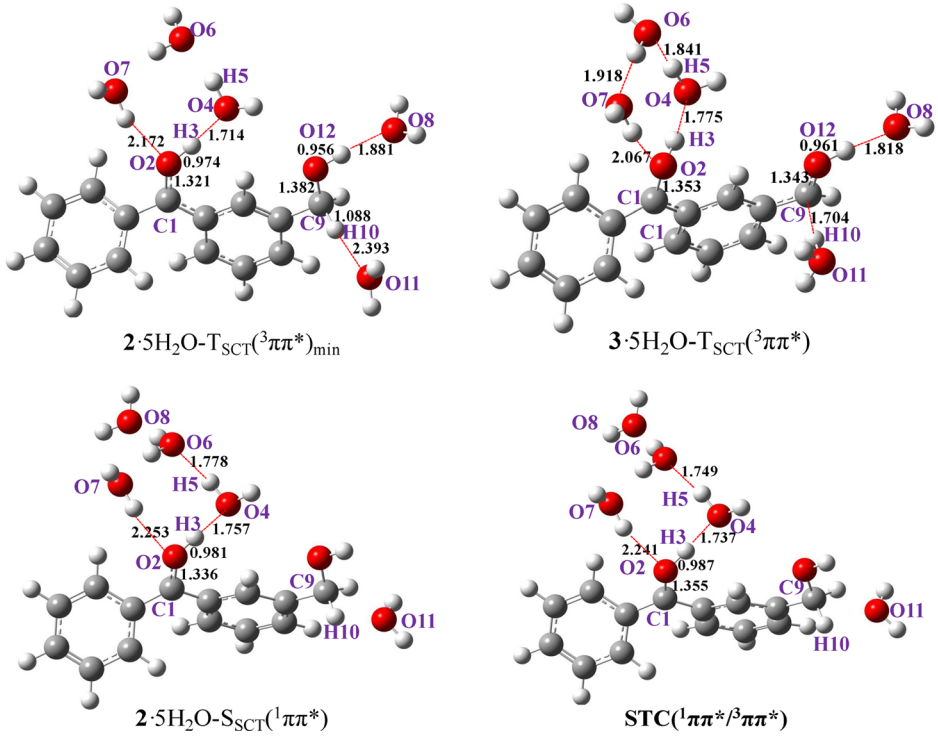

Figure 3. Schematic stationary structures of **2**·5H$_2$O in the $S_{SCT}(^1\pi\pi^*)$ state and intersection structure of STC($^1\pi\pi^*/^3\pi\pi^*$) for the **2**·5H$_2$O complex as well as the local minima of **2**·5H$_2$O and **3**·5H$_2$O complex in the $T_{SCT}(^3\pi\pi^*)$ state, along with the key bond lengths (in Å) at the CAS(14e/11o)/6-31G* level of theory.

and O(4)···H(5) hydrogen bonds, pave a favorable way for the proton transfer from the aqueous solution to the O(2) atom.

One water molecule of H$_2$O(4) is introduced to function as a bridge to assist the proton transfer, while two water molecules [H$_2$O(7) and H$_2$O(8)] are used for stabilization of the hydroxonium ion [H$_2$O(6)]. As illustrated in Figure 2, 243 nm UV light takes the system of **1**·5H$_2$O to instantaneously populate in the FC of the $S_{SCT}(^1\pi\pi^*)$ state. This excitation significantly results in an abundant gathering of negative charge around the center of the carbonyl group. The proton in the solution is easily attracted by O(2) in the $S_{SCT}(^1\pi\pi^*)$ state to facilitate an excited state intermolecular proton transfer. The **1**·5H$_2$O from the $S_{SCT}(^1\pi\pi^*)$ excited state rapidly decays to a local minimum that is ∼115.3 kcal/mol above the S_0 energy minimum. The potential well of this local minimum is extremely shallow, where a barrier of only ∼3.4 kcal/mol is encountered, leading to a downhill relaxation pathway. This barrier (∼3.4 kcal/mol) is smaller than that of the ESIPT reaction (∼9.9 kcal/mol) in the same excited state of ketoprofen assisted by two water molecules[23] but larger than that of barrierless excited state intramolecular proton transfer of *o*-acetylphenylacetic acid showing a short donor/acceptor distance (1.655 Å) without water participation.[25] This indicates that the magnitude of the barrier is closely related to the distance between the donor and acceptor of proton transfer.

Once **1**·5H$_2$O overcomes the small barrier, the H(3)−O(2) distance is sharply shortened to 1.13 Å from 1.64 Å in the maximum of the energy curve while the O(4)−H(5) distance changes to 0.98 Å from 1.27 Å. This indicates that the loss of the proton H(3) for the water molecule [H$_2$O(4)] is compensated by the proton H(5), and this quantitatively simulates the photoinduced protonation reaction of **1** in aqueous solution. It should be noted that the distance between the donor and the acceptor for the proton transfer may be shorter in a "real" solution environment than that mimicked in this work. In this case, the barrier should be lower than the ∼3.4 kcal/mol that is estimated according to the present water complex model. The photoinduced protonation reaction is a fast process with a tiny barrier or barrierless in the short-distance charge transfer excited state $S_{SCT}(^1\pi\pi^*)$. Obviously, the ultrafast ESIPT reaction proceeds in an anti-Kasha's rule manner.[33] We present detailed discussions in section 3 of Supporting Information based on the extended calculations and comparisons with our previous works.[11,17,23−25,34−36]

As shown in Figure 2, after crossing this tiny barrier (∼3.4 kcal/mol), the energy curve falls to a flat valley where the energy level ranges from 94.2 (D_{O4-H3} = 1.2 Å) to 86.5 kcal/mol (D_{O4-H3} = 1.8 Å) to produce the enol form of $S_{SCT}(^1\pi\pi^*)$-*E*. The intermediate **2** is eventually formed by a structural adjustment (see Figure 3). A Mulliken population analysis shows that the sum of the charge localized in the phenylcarbinol moiety increases from +0.02 in **1**·5H$_2$O to +0.80 in intermediate **2**·5H$_2$O. This indicates that a positive charge center is generated around the aromatic ring of the phenylcarbinol moiety for intermediate **2** by the above excited state protonation reaction, which is in good agreement with the nature of the reactive intermediate assigned by Wan[11,13] and Phillips.[17]

Deprotonation Reaction in the Triplet State. It has been well-established that $^1n,\pi^* \rightarrow {}^3\pi,\pi^*$ intersystem crossing is efficient for aromatic carbonyl compounds, leading to further photochemical reactions in the triplet state.[34,35,37,44] The singlet and triplet surface crossing for the **2**·5H$_2$O species was found by using state-averaged CASSCF computations with Slater determinants. This stationary point was identified as a $^1\pi\pi^*$ and $^3\pi\pi^*$ singlet and triplet crossing by careful configuration

dx.doi.org/10.1021/jo4008783 | J. Org. Chem. 2013, 78, 5677−5684

analyses and was therefore referred to as STC($^1\pi\pi^*/^3\pi\pi^*$). The spin−orbit coupling of STC($^1\pi\pi^*/^3\pi\pi^*$) is calculated to be 1.3 cm^{-1}, which is consistent with the order of magnitude of 0.3−0.001 kcal/mol (104.9−0.3 cm^{-1}) expected for such photochemistry.[33] According to the El-Sayed selection rules, the $^1\pi,\pi^* \rightarrow {}^3\pi,\pi^*$ transition is considered to be forbidden in zero order, while the $^1n,\pi^* \rightarrow {}^3\pi,\pi^*$ intersystem crossing is allowed. The optimization of the singlet and triplet crossing for the STC($^1\pi\pi^*/^3\pi\pi^*$) of **2**·5H_2O determined a stationary point at the 1.355 Å C(1)−O(2) distance, in which the singlet and triplet states have an almost degeneracy energy. Such a small energy gap allows the $^1\pi,\pi^* \rightarrow {}^3\pi,\pi^*$ transition to become favorable by introduction of vibrational coupling in the second order approximation.[33] As shown in Figure 3, apart from the hydrogen bonding around intermediate **2**, the STC-($^1\pi\pi^*/^3\pi\pi^*$) structure is not changed too much with the exception of the C(1)−O(2) bond that is elongated by 0.019 Å, as compared with that of **2**·5H_2O-$S_{SCT}(^1\pi\pi^*)$. The singlet−triplet crossing of STC($^1\pi\pi^*/^3\pi\pi^*$) is energetically located at ∼79.5 kcal/mol above the minimum of the S_0 state.

As illustrated in Figure 4, STC($^1\pi\pi^*/^3\pi\pi^*$) relays the **2**·5H_2O of $S_{SCT}(^1\pi\pi^*)$ intersystem crossing to a local minimum

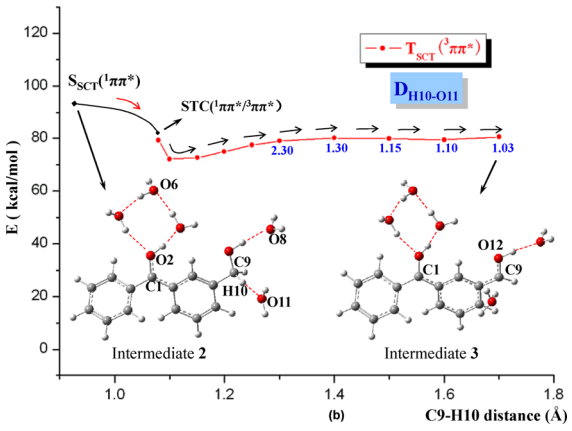

Figure 4. CEP for deprotonation of intermediate **2**·5H_2O in the $T_{SCT}(^3\pi\pi^*)$ state along the reaction coordinate of C(9)−H(10) [or H(10)−O(11)] distance obtained at the CAS (14e/11o)/CASPT2/6-31G* level of theory.

of the $T_{SCT}(^3\pi\pi^*)$ state that is ∼72.1 kcal/mol above the zero level energy of the S_0 state. The deuterium isotope effect experiment conducted by Wan and co-workers[11] suggested that deprotonation of the benzylic proton H(10) of **2** to form a biradical intermediate is an integral part of the mechanism.[11,17] To examine this mechanism, the CEP of the proton transfer of H(10) from C(9) to $H_2O(11)$ was mapped along the reaction coordinate of C(9)−H(10) [or H(10)−O(11) ($D_{H10-O11}$)] distance in $T_{SCT}(^3\pi\pi^*)$ state. In order to obtain a more reasonable model for our calculations, one water molecule of $H_2O(8)$ that will be the potential proton acceptor in following the water-assisted self-redox reaction is moved from afar to form hydrogen bonding with intermediate **2** (see Figure 4), and then unconstrained optimizations in the $T_{SCT}(^3\pi\pi^*)$ state were carried out to locate the structure of the reactant for deprotonation reaction in the triplet state. Adjusting the spatial location of the water molecule to mimic the solvent environment and not the introduction of an extra water molecule was done to ensure that there are a consistent number of molecules for all of the calculations done on the different reaction pathways.

As shown in Figure 4, an ∼8.0 kcal/mol barrier is encountered when the system evolves from the minimum of **2**·5H_2O-$T_{SCT}(^3\pi\pi^*)$ and then reaches an energy barrier at the 1.4−1.7 Å C(9)−H(10) distance. With the departure of the proton H(10), the negative charge left combines with the positive charge around the aromatic ring of the phenylcarbinol to produce a neutral triplet species denoted as intermediate **3** that is energetically ∼80.5 kcal/mol above the zero level energy of the S_0 state. An electronic population analysis indicates that the two singly occupied electrons of **3** distribute in the regions of the C(1) and C(9) atoms, respectively. This indicates that intermediate **3** adopts a biradical configuration that is in good agreement with previous assignment on the basis of experimentally observed results.[23,45−47] The lifetime of **3** was observed to be ∼430 ns under open air conditions and significantly decreased to ∼60 ns in an oxygen-purging experiment,[17] which confirms the nature of **3** to be a triplet state. For the configuration of **3**·5H_2O, the absorption band with the largest oscillator strength is calculated to vary with the model used for the hydrogen bonding around **3** and lies at ∼55.5 to ∼62.9 kcal/mol above the zero level energy of **3**·5H_2O. This is close to the λ_{max} of 525 nm (54.5 kcal/mol) transient absorption observed experimentally for the biradical species.[11] The long-lived triplet biradical of **3** functions as an effective precursor for the subsequent photoredox reaction.

As shown in Figure 3, the C(9)−H(10) distance is elongated from 1.09 Å in **2**·5H_2O-$T_{SCT}(^3\pi\pi^*)_{min}$ to ∼1.70 Å in the minimum of **3**·5H_2O-$T_{SCT}(^3\pi\pi^*)$, while the C(9)−O(12) distance is shortened from 1.38 Å to 1.34 Å, which indicates that some double bond character develops. It seems that the deprotonation from O(12) to form a C(9)−O(12) carbonyl group is a subsequent process. However, this reaction in the $T_{SCT}(^3\pi\pi^*)$ state was calculated to have more than 26.0 kcal/mol barrier (see section 4 in Supporting Information), which rules out the possibility of direct formation of C(9)−O(12) carbonyl group in the $T_{SCT}(^3\pi\pi^*)$ state. In contrast with this, the quenching time of intermediate **3** was observed to vary with pH of the aqueous solution ($\tau_{(pH\ 7)}$ = 9.5 μs, $\tau_{(pH\ 2)}$ = 60 ns),[11] which indicates that protonation of **3** is a precondition for the photoredox reaction. Therefore, as an alternative relaxation channel, the protonation of C(1) in biradical intermediate **3** was explored as a subsequent process.

Water-Assisted Self-Redox Reaction. As discussed above, the protonation of the benzhydrol carbon C(1) of the biradical intermediate **3** is a precondition for the subsequent self-redox reaction. However, it is difficult to occur for the direct proton transfer due to a large spatial distance (∼5.0 Å) between the acceptor C(1) and the donor $H_3O^+(10)$ that has been generated in the above triplet state deprotonation reaction. Therefore, water assistance is required to bridge the proton transfer from the donor of $H_3O^+(10)$ to the acceptor C(1). The water molecule $H_2O(6)$ is moved to the vicinity of C(1) and $H_3O^+(10)$ and then undergoes unconstrained optimizations in the $T_{SCT}(^3\pi\pi^*)$ state, producing the reactant for the self-redox reaction. As previously mentioned, this adjustment of the position of the water molecule could maintain a consistent number of molecules in the system when exploring the different pathways.

As shown in Figure 5, the alternation of the hydrogen bonding pattern leads to a more stable local minimum that is ∼11.9 kcal/mol lower than that of the former biradical

dx.doi.org/10.1021/jo4008783 | J. Org. Chem. 2013, 78, 5677−5684

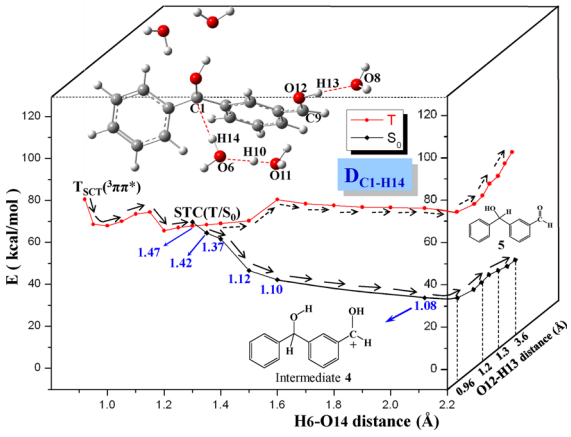

Figure 5. CEP for the self-redox reaction of intermediate **3** is shown via two serial processes, protonation with benzhydrol carbon C(1) producing intermediate **4** and deprotonation from benzylic oxygen O(12) yielding the final product **5** at the CASPT2//CAS(14e/11o)/6-31G* level of theory.

($\mathbf{3}\cdot5H_2O$-$T_{SCT}(^3\pi\pi^*)$) in energy. The elongation of the O(6)−H(14) distance results in an uphill energy curve and first overcomes a moderate barrier (~5.8 kcal/mol) at a 1.15 Å O(6)−H(14) distance and eventually reaches the maximum with a 14.8 kcal/mol barrier at a 1.60 Å O(6)−H(14) distance in the triplet state pathway. This high barrier almost closes the adiabatic reaction channel in the triplet state. However, another singlet−triplet crossing [STC(T/S_0)] between $T_{SCT}(^3\pi\pi^*)$ and the ground state was found at a 1.30 Å O(6)−H(14) distance (for its schematic structure see Figure 6), which opens a spin-forbidden reaction channel for the proton transfer from an aqueous solution to C(1). The spin−orbital coupling for STC(T/S_0) is only 0.7 cm^{-1} which is consistent with the $T(^3\pi,\pi^*) \rightarrow S_0$ transition being forbidden in the zero order approximation.[33] As discussed above, the efficient vibronic coupling in combination with a small T_1-S_0 energy gap (~2.7 kcal/mol) facilitates the occurrence of intersystem crossing relaxing the system to the ground state. Unlike the energy curve in the triplet state, a downhill potential energy profile on the spin-forbidden pathway allows a fast protonation reaction leading to the ground state intermediate of **4** that has 33.5 kcal/mol energies with respect to the zero level energy of the S_0 minimum. The vertical excitation energy for the transition with the largest oscillator strength was calculated to be at ~91.8 kcal/mol (~312 nm) above the zero level energy of the ground state $\mathbf{4}\cdot5H_2O$. This is very close to the λ_{max} 325 nm (88.0 kcal/mol) transient absorption band observed experimentally.[11]

Apart from the formation of the C1−H14 bond, the most striking structural change is associated with the C(9)−O(12) bond length during the above process. As depicted in Figure 6, the C(9)−O(12) bond length is shortened from 1.37 Å in STC(T/S_0) to 1.27 Å in intermediate $\mathbf{4}\cdot5H_2O$-S_0 that exhibits obvious double bond character. Meanwhile, the O(12)−H(13) bond is elongated from 0.96 Å to 1.01 Å, while the H(13)···O(8) distance is shortened from 1.81 Å to 1.65 Å in this process. In addition, a Mulliken charge population analysis shows that ~0.3 positive charge resides on the C(9) in the evolvement from STC(T/S_0) to intermediate **4**, generating a positive charge center around C(9). All of these changes mentioned above indicate the C(9)−O(12) bond of intermediate **4** already exhibits the typical character of a carbonyl group, and the photoinduced oxidation reaction is almost accomplished except for the deprotonation of H(13) from the carbonyl group C(9)−O(12). Therefore, the deprotonation reaction proceeds easily with the assistance of a water molecule $H_2O(8)$ that functions as a proton acceptor. As shown in Figure 5, an energy platform ranging from 37.0 to 39.1 kcal/mol is found to be predominant for the proton [H(13)] transfer from O(12) to O(8) with the increase of the O(12)−H(13) distance. This reveals that the last step of deprotonation is a fast and highly efficient process. With the departure of proton H(13), the final product **5** is produced finally to achieve the photoinduced self-redox reaction assisted by water molecules.

CONCLUSIONS

In this work, we report the mechanism of th water-assisted self-photoredox of 3-(hydroxymethyl) benzophenone **1** via three sequential reactions: an excited-state intermolecular proton transfer, a photoinduced deprotonation, and a self-redox reaction (see Scheme 2). Triggered by 243 nm photoexcitation, an excited-state intermolecular proton transfer takes place to capture a proton from the acidic aqueous solution to produce intermediate **2**. Following this, the wavepacket of the $S_{SCT}(^1\pi\pi^*)$ state relaxes to the $^3\pi\pi^*$ state via an efficient intersystem crossing followed by deprotonation with a moderate barrier of ~8.0 kcal/mol to yield the triplet biradical intermediate **3**. After overcoming another moderate barrier (~5.8 kcal/mol) in the $^3\pi\pi^*$ state, the intermediate **3** relaxes to the singlet−triplet crossing of STC(T/S_0) that allows an efficient spin-forbidden decay to the ground state. A subsequent self-redox reaction aided by water molecules occurs with a tiny barrier or without a barrier in the ground state via two serial processes, protonation of the benzhydrol carbon to produce intermediate **4** and then deprotonation from the benzylic

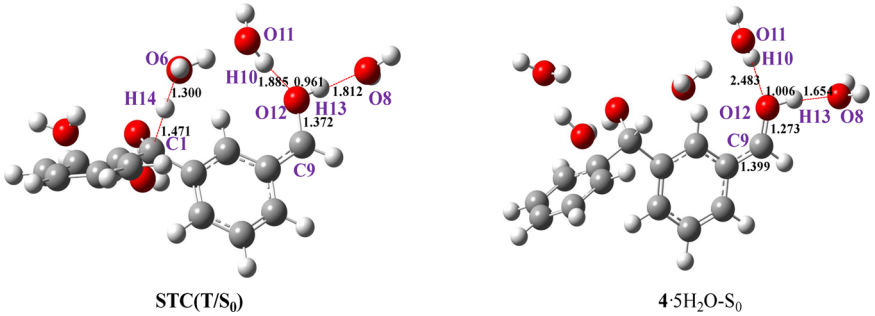

Figure 6. Schematic depictions of the structures for the singlet−triplet crossing STC(T/S_0) and the $\mathbf{4}\cdot5H_2O$-S_0 complex along with the key bond lengths (in Å) determined at the CAS(14e/11o)/6-31G* level of theory.

dx.doi.org/10.1021/jo4008783 | J. Org. Chem. 2013, 78, 5677−5684

Scheme 2. Plausible Mechanism the Water-Assisted Self-Photoredox of 3-(Hydroxymethyl) Benzophenone (1) Proposed by Theoretical Simulations of *ab Initio* Multiconfigurational Perturbation Theory

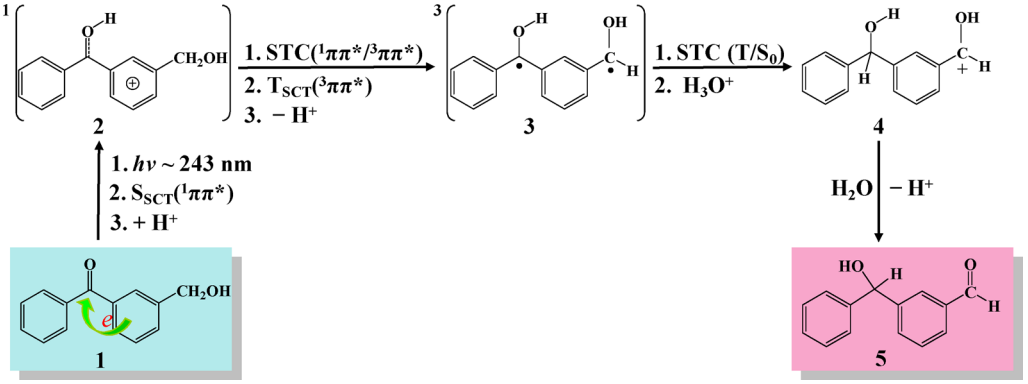

oxygen to yield the final product 3-formylbenzhydrol **5**. The H_2O molecules were found to function respectively as donor, water bridge, and acceptor to assist proton transfer, which indicates that the participation of water molecules is an essential precondition in these reactions. For the configurations of the intermediates **3** and **4**, the absorption bands with the largest oscillator strengths are calculated energetically to correspond to 515 and 312 nm, respectively, and these values are in good agreement with the λ_{max} 525 and 325 nm transient absorption bands observed experimentally for the photolysis of **1** in an acidic (pH <3) aqueous solution. These indicate that the proposed reaction mechanisms for an unusual photochemistry of water-assisted self-photoredox of 3-(hydroxymethyl) benzophenone are reasonable on the basis of the present computational results. Our present computational efforts provide a clear and feasible mechanism for this complicated photoredox reaction and will help with understanding of the photochemistry of benzophenone and its analogous compounds in aqueous solution.

■ ASSOCIATED CONTENT

Supporting Information

Discussions, computational details, figures, tables and Cartesian coordinates. This material is available free of charge via the Internet at http://pubs.acs.org.

■ AUTHOR INFORMATION

Corresponding Author

*E-mail: xuebochen@bnu.edu.cn; fangwh@bnu.edu.cn; phillips@hku.hk.

Notes

The authors declare no competing financial interest.

■ ACKNOWLEDGMENTS

This work has been supported by FANEDD 200932, NCET-11-0030, and NSFC20973025 (X.C.); NSFC20720102038 and Major State Basic Research Development Programs 2011CB808503 (W.F.), and the Research Grants Council of Hong Kong (HKU 7048/11P) (D.L.P.)

■ REFERENCES

(1) Sakamoto, M.; Cai, X. C.; Kim, S. S.; Fujitsuka, M.; Majima, T. *J. Phys. Chem. A* **2007**, *111*, 223−229.
(2) (a) Scaiano, J. C. *J. Photochem.* **1973−1974**, *2*, 81−118. (b) Matinez, L. J.; Scaiano, J. C. *J. Am. Chem. Soc.* **1997**, *119*, 11066−11070. (c) Lukeman, M.; Scaiano, J. C. *J. Am. Chem. Soc.* **2005**, *127*, 7698−7699.
(3) Shah, B. K.; Neckers, D. C. *J. Am. Chem. Soc.* **2004**, *126*, 1830−1835.
(4) Matsushita, Y.; Kajii, Y.; Obi, K. *J. Phys. Chem.* **1992**, *96*, 6566−6570.
(5) Ariel, S.; Ramamurthy, V.; Scheffer, J. R.; Trotter, J. *J. Am. Chem. Soc.* **1983**, *105*, 6959−6960.
(6) Zimmerman, H. E.; Schuster, D. I. *J. Am. Chem. Soc.* **1962**, *84*, 4527−4540.
(7) Yabumoto, S.; Sato, S.; Hamaguchi, H. *Chem. Phys. Lett.* **2005**, *416*, 100−103.
(8) Okutsu, T.; Muramatsu, H.; Horiuchi, H.; Hiratsuka, H. *Chem. Phys. Lett.* **2005**, *404*, 300−303.
(9) (a) An, H. Y.; Kwok, W. M.; Ma, C. S.; Guan, X. G.; Kan, J. T. W.; Toy, P. H.; Phillips, D. L. *J. Org. Chem.* **2010**, *75*, 5837−5851. (b) Ma, C. S.; Zuo, P.; Kwok, W. M.; Chan, W. S.; Kan, J. T. W.; Toy, P. H.; Phillips, D. L. *J. Org. Chem.* **2004**, *69*, 6641−6657. (c) Du, Y.; Xue, J. D.; Li, M. D.; Phillips, D. L. *J. Phys. Chem. A* **2009**, *113*, 3344−3352.
(10) Hou, Y. Y.; Huck, L. A.; Wan, P. *Photochem. Photobiol. Sci.* **2009**, *8*, 1408−1415.
(11) Mitchell, D.; Lukeman, M.; Lehnherr, D.; Wan, P. *Org. Lett.* **2005**, *15*, 3387−3389.
(12) Lukeman, M.; Xu, M. S.; Wan, P. *Chem Commun.* **2002**, *2*, 136−137.
(13) Huck, L. A.; Wan, P. *Org. Lett.* **2004**, *11*, 1797−1799.
(14) (a) Zimmerman, H. E. *J. Am. Chem. Soc.* **1995**, *117*, 8988−8991. (b) Zimmerman, H. E. *J. Phys. Chem. A* **1998**, *102*, 5616−5621.
(15) Ramseier, M.; Senn, P.; Wirz, J. *J. Phy. Chem. A* **2003**, *107*, 3305−3315.
(16) Du, Y.; Ma, C. S.; Kwok, W. M.; Xue, J. D.; Phillips, D. L. *J. Org. Chem.* **2007**, *72*, 7148−7156.
(17) Ma, J. N.; Li, M. D.; Phillips, D. L.; Wan, P. *J. Org. Chem.* **2011**, *76*, 3710−3719.
(18) Ljunggren, B. *Photodermatology* **1985**, *2*, 3−9.
(19) Przybilla, B.; Schwab-Przybilla, U.; Ruzicka, T.; Ring, J. *Photodermatology* **1987**, *4*, 73−78.
(20) Buntinx, G.; Poizat, O. *Laser Chem.* **1990**, *10*, 333−347.
(21) Suzuki, T.; Okita, T.; Osanai, Y.; Ichimura, T. *J. Phys. Chem. B* **2008**, *112*, 15212−15216.
(22) Ma, C. S.; Kwok, W. M.; An, H. Y.; Fu, M. Y.; Toy, P. H.; Phillips, D. L. *Chem.—Eur. J.* **2010**, *16*, 5102−5118.
(23) Xu, Y. C.; Chen, X. B.; Fang, W. H.; Phillips, D. L. *Org. Lett.* **2011**, *13*, 5472−5475.
(24) Chen, X. B.; Ma, C. S.; Phillips, D. L.; Fang, W. H. *Org. Lett.* **2010**, *12*, 5108−5111.
(25) Ding, L.; Chen, X. B.; Fang, W. H. *Org. Lett.* **2009**, *11*, 1495−1498.
(26) Ding, L.; Fang, W. H. *J. Org. Chem.* **2010**, *75*, 1630−1636.

(27) Ding, L.; Shen, L.; Chen, X. B.; Fang, W. H. *J. Org. Chem.* **2009**, *74*, 8956−8962.
(28) (a) Roos, B. O.; Taylor, P. R.; Siegbahn, P. E. M. *Chem. Phys.* **1980**, *48*, 157. (b) Ruedenberg, K.; Schmidt, M.; Gilbert, M. M.; Elbert, S. T. *Chem. Phys.* **1982**, *71*, 41−49.
(29) Werner, H. J.; Knowles, P. J. *J. Chem. Phys.* **1985**, *82*, 5053−5063.
(30) (a) Andersson, K.; Malmqvist, P. Å.; Roos, B. O.; Sadlej, A. J.; Wolinski, K. *J. Phys. Chem.* **1990**, *94*, 5483−5488. (b) Andersson, K.; Malmqvist, P. Å.; Roos, B. O. *J. Chem. Phys.* **1992**, *96*, 1218−1226.
(31) Frisch, M. J.; Trucks, G. W.; Schlegel, H. B.; Scuseria, G. E.; Robb, M. A.; Cheeseman, J. R.; Montgomery Jr., J. A.; Vreven, T.; Kudin, K. N.; Burant, J. C.; Millam, J. M.; Iyengar, S. S.; Tomasi, J.; Barone, V.; Mennucci, B.; Cossi, M.; Scalmani, G.; Rega, N.; Petersson, G. A.; Nakatsuji, H.; Hada, M.; Ehara, M.; Toyota, K.; Fukuda, R.; Hasegawa, J.; Ishida, M.; Nakajima, T.; Honda, Y.; Kitao, O.; Nakai, H.; Klene, M.; Li, X.; Knox, J. E.; Hratchian, H. P.; Cross, J. B.; Adamo, C.; Jaramillo, J.; Gomperts, R.; Stratmann, R. E.; Yazyev, O.; Austin, A. J.; Cammi, R.; Pomelli, C.; Ochterski, J. W.; Ayala, P. Y.; Morokuma, K.; Voth, G. A.; Salvador, P.; Dannenberg, J. J.; Zakrzewski, V. G.; Dapprich, S.; Daniels, A. D.; Strain, M. C.; Farkas, O.; Malick, D. K.; Rabuck, A. D.; Raghavachari, K.; Foresman, J. B.; Ortiz, J. V.; Cui, Q.; Baboul,A. G.; Clifford, S.; Cioslowski, J.; Stefanov, B. B.; Liu, G.; Liashenko, A.; Piskorz, P.; Komaromi, I.; Martin, R. L.; Fox, D. J.; Keith, T.; Al-Laham, M. A.; Peng, C. Y.; Nanayakkara, A.; Challacombe, M.; Gill, P. M. W.; Johnson, B.; Chen, W.; Wong, M. W.; González, C.; Pople, J. A. *Gaussian03, Revision D.02*, Gaussian, Inc.: Pittsburgh, PA, 2004.
(32) Aquilante, F.; De Vico, L.; Ferré, N.; Ghigo, G.; Malmqvist, P.-å.; Neogrády, P.; Pedersen, T. B.; Pitoňák, M.; Reiher, M.; Roos, B. O.; Serrano-Andrés, L.; Urban, M.; Veryazov, V.; Lindh, R. *J. Comput. Chem.* **2010**, *31*, 224−247.
(33) (a) Turro, N. J. *Modern Molecular Photochemistry*; University Science Books: Sausalito, 1991. (b) Kasha, M. *Discuss. Faraday Soc.* **1950**, *9*, 14−19.
(34) Chen, X. B.; Fang, W. H. *J. Am. Chem. Soc.* **2004**, *126*, 8976−8980.
(35) Fang, W. H. *Acc. Chem. Res.* **2008**, *41*, 452−457.
(36) Chen, X. B.; Fang, W. H. *Chem. Phys. Lett.* **2002**, *361*, 473−482.
(37) Zepp, R. G.; Gumz, M. M.; Miller, W. L.; Gao, H. *J. Phys. Chem. A* **1998**, *102*, 5716−5723.
(38) Singhal, N.; Koner, A. L.; Mal, P.; Venugopalan, P.; Nau, W. M.; Moorthy, J. N. *J. Am. Chem. Soc.* **2005**, *127*, 14375−14382.
(39) Ma, C. S.; Kwok, W. M.; Chan, W. S.; Du, Y.; Kan, J. T. W.; Toy, P. H.; Phillips, D. L. *J. Am. Chem. Soc.* **2006**, *128*, 2558−2570.
(40) Schneider, M. H.; Tran, Y.; Tabeling, P. *Langmuir* **2011**, *27* (3), 1232−1240.
(41) Deng, J.; Wang, L.; Liu, L.; Yang, W. *Prog. Polym. Sci.* **2009**, *34*, 156−193.
(42) Dorman, G.; Prestwich, G. D. *Biochemistry* **1994**, *33*, 5661−5673.
(43) Chen, X. B.; Ma, C. S.; Kwok, W. M.; Guan, X. G.; Du, Y.; Phillips, D. L. *J. Phys. Chem. B* **2007**, *111*, 11832−11842.
(44) Stensrud, K.; Noh, J.; Kandler, K.; Wirz, J.; Heger, D.; Givens, R. S. *J. Org. Chem.* **2009**, *74*, 5219−5227.
(45) Chuang, Y. P.; Xue, J. D.; Li, M. D.; Du, Y.; An, H. Y.; Phillips, D. L. *J. Phys. Chem. B* **2009**, *113*, 10530−10539.
(46) Li, M. D.; Du, Y.; Chuang, Y. P.; Xue, J. D.; Phillips, D. L. *Phys. Chem. Chem. Phys.* **2010**, *12*, 4800−4808.
(47) Li, M. D.; Yeung, C. S.; Guan, X. G.; Ma, J. N.; Li, W.; Ma, C. S.; Phillips, D. L. *Chem.—Eur. J.* **2011**, *17*, 10935−10950.